

Subpicosecond plasma dynamics and absorption saturation in GaAs

J. Collet

*Laboratoire de Physique des Solides, Institut National des Sciences Appliquées, avenue de Rangueil,
31077 Toulouse Cédex, France*

J. L. Oudar

Laboratoire de Bagnex, Centre National des Télécommunications, 92220 Bagnex, France

T. Amand

*Laboratoire de Physique des Solides, Institut National des Sciences Appliquées, avenue de Rangueil,
31077 Toulouse Cédex, France*

(Received 20 March 1986; revised manuscript received 3 June 1986)

We develop a model calculation to describe the athermal dynamics of an electron-hole plasma in a direct-gap semiconductor under subpicosecond optical excitation. The computations are especially focused on the problem of optical absorption saturation in such a regime. The model fits perfectly recent experimental results on GaAs. Carrier dampings (due to LO-phonon-carrier and carrier-carrier scatterings) are calculated as a function of the electron states distribution. We show that the carrier dampings first increase quickly when the plasma density is increased under laser excitation ($\rho < 5 \times 10^{16} \text{ cm}^{-3}$) but thereafter decay due to the plasma degeneracy and the screening effect which reduces the amplitude of the renormalized interactions. The occurrence of the absorption saturation in subpicosecond pulse experiments is considered in GaAs for excitation photons, the energy of which ranges from 1.538 to 1.61 eV.

I. INTRODUCTION

With the permanent progress of laser sources, the experimental investigation of athermal systems such as electron-hole plasma or optical phonons is now possible on a picosecond or even a subpicosecond time scale by gain-absorption or Raman spectroscopy.¹⁻⁴ The kinetics of such a regime, which are athermal both for carriers and phonons, are mainly controlled by the efficiency of the different scattering processes (i.e., carrier-carrier scatterings and carrier-phonon inelastic scatterings), which in their turn depend also on the plasma density. The plasma dynamics are governed by nonlinear equations under conditions of strong optical pumping. The full general treatment of plasma dynamics equations is extremely difficult so that a compromise must be chosen between the refinement in the description of the scattering (dielectric function) and the refinement in the theory of nonequilibrium kinetic equations. We discussed the choice of possible equations and the development of a model of athermal plasma dynamics in a previous work.⁵ Let us recall that at least three kinetic equations must be considered to account for the transient athermal regime on a subpicosecond time scale: one for electrons in the conduction band, one for holes in the valence band, and one for the LO phonons.^{5,6} It is now well known that the LO-phonon distribution becomes also athermal under strong excitation in picosecond or subpicosecond pulse experiments.³⁻⁴ Among the possible nonlinear effects in the subpicosecond regime, we consider especially in the present work the optical absorption saturation or, in other words, the increase of the material transmission under

strong excitation. This effect occurs because the conduction and valence states, which are resonant with the probe photons, become significantly populated. The following degeneracy condition holds:

$$1 - f_c(\mathbf{k}_p) - f_v(\mathbf{k}_p) \sim 0. \quad (1)$$

Here, \mathbf{k}_p is the wave vector of photons interacting with the material. f_c and f_v are the distribution functions of electrons in the conduction band and holes in the valence band, respectively. It must be stressed that the fulfillment of this condition (1), which monitors the amplitude (and the broadening) of the absorption saturation, depends critically on the efficiency of the different collision processes that scatter the carriers generated by the excitation light out of their initial state (wave vector \mathbf{k}_p). For instance, at low excitation, the only scattering process to consider on a picosecond time scale is the inelastic scattering by LO phonons. Under strong excitation, carrier-carrier scatterings become dominant and must also be taken into account. As a result, absorption saturation experiments are a good tool for testing the models of athermal plasma dynamics, especially the efficiency of the renormalization effects (induced by the generated plasma) on the quasiparticle interactions. It must be also stressed that absorption saturation is of great interest in relation to the realization of all-solid-state saturable absorbers for picosecond laser mode locking. In Sec. III, we compare recent experimental results published by one of us² with our model and discuss the screening efficiency through an effective screening wave vector. Carrier dampings are calculated and discussed. In Sec. IV, we investigate the possible occurrence of the absorption saturation in GaAs for excitation pho-

tons, the energy of which ranges from 1.538 to 1.61 eV. We recall first the kinetic equations.

II. KINETIC EQUATIONS

The problem of plasma dynamics on a subpicosecond time scale must be worked out in a general framework of nonequilibrium statistical mechanics. Very general quantum-mechanical treatments have been developed for that purpose, but the quantitative application to real problems leads generally to quasi-inextricable mathematical difficulties in partial differential and integral equations originating (among several causes) in non-Markovian aspects. We refer here to the following general treatments.⁷⁻⁹ No analytical solution is expected for a physical system very far from the thermodynamical equilibrium and the computational treatment of non-Markovian kinetic equations (including dynamical polarization effects) remains beyond our computer capabilities. We choose to write down simple Markov-like equations. So we retain the following set of equations:^{5,10}

$$\begin{aligned} \frac{d}{dt}f_c(\mathbf{k}) &= \left. \frac{df}{dt} \right|_{cc} + \left. \frac{df}{dt} \right|_{cv} + \left. \frac{df}{dt} \right|_{c,LO} + g_c(\mathbf{k}, t), \\ \frac{d}{dt}f_v(\mathbf{k}) &= \left. \frac{df}{dt} \right|_{vc} + \left. \frac{df}{dt} \right|_{vv} + \left. \frac{df}{dt} \right|_{v,LO} + g_v(\mathbf{k}, t), \quad (2) \\ \frac{d}{dt}b_{LO}(\mathbf{q}) &= \left. \frac{db}{dt} \right|_{LO,c} + \left. \frac{db}{dt} \right|_{LO,v}. \end{aligned}$$

$f_c(\mathbf{k})$, $f_v(\mathbf{k})$, and $b_{LO}(\mathbf{q})$ are, respectively, the distribution functions of electrons in the conduction band, holes in the valence band, and LO phonons. No TO-phonon equation is considered in system (2), although there is no difficulty in principle with taking it into account. The reason is that the model calculation will be compared to experimental results on GaAs. In this material, carriers are more strongly coupled to LO phonons than to TO phonons. As a result, the TO-distribution function is expected to be weakly disturbed from its equilibrium value when the optical pumping energy $\hbar\omega$ is close to the band-gap energy E_G (i.e., when the condition $\hbar\omega - E_G < \hbar\omega_{TO}$ holds; here $\hbar\omega_{TO}$ is the TO-phonon energy). This is *a posteriori* justified by the results of the calculation. We dropped the diffusion terms so that Eqs. (2) hold for an homogeneous (or a quasihomogeneous) electron-hole plasma. Such plasma can be easily generated using two-photon absorption,¹¹ or in case of one-photon excitation, if the condition $\alpha(h\nu)L < 1$ holds (here, α is the absorption coefficient, $h\nu$ is the pump photon energy, and L is the sample thickness). Recombination terms are not significant on the time range investigated here, typically less than 2 ps. They will not be considered. We recall that the right-hand-side contributions of Eqs. (2) represent the scattering rates due to carrier-carrier collisions and also to the inelastic carrier-LO-phonon scatterings. g_v and g_c are, respectively, the generation rates of holes in the valence band and electrons in the conduction band resulting from the laser pulse absorption. Each scattering term $(df/dt)|_{\alpha\beta}$ can be cast as follows:

$$\left. \frac{df}{dt} \right|_{\alpha\beta} = - \left. \frac{df}{dt} \right|_{\alpha\beta}^{\text{out}} + \left. \frac{df}{dt} \right|_{\alpha\beta}^{\text{in}}. \quad (3)$$

$(df/dt)|_{\alpha\beta}^{\text{out}}$ accounts for the processes that scatter the carrier out of its initial state, while $(df/dt)|_{\alpha\beta}^{\text{in}}$ accounts for the processes that scatter carriers into the k state. The “in” and “out” contributions read

$$\begin{aligned} \left. \frac{d}{dt}f \right|_{\alpha\beta}^{\text{in}} &= [1 - f_\alpha(\mathbf{k}, t)] \sum_q S_{\alpha\beta}^{\text{in}}(\mathbf{k}, \mathbf{k} - \mathbf{q}, \Delta E) f_\alpha(\mathbf{k} - \mathbf{q}, t), \\ \left. \frac{d}{dt}f \right|_{\alpha\beta}^{\text{out}} &= f_\alpha(\mathbf{k}, t) \sum_q S_{\alpha\beta}^{\text{out}}(\mathbf{k}, \mathbf{k} - \mathbf{q}, \Delta E) [1 - f_\alpha(\mathbf{k} - \mathbf{q}, t)]. \end{aligned} \quad (4)$$

Such equations hold in degenerate plasma, which is absolutely necessary for describing in the next section saturation absorption experiments. For the carrier-carrier interaction, $S_{\alpha\beta}^{\text{in}}(\mathbf{k}, \mathbf{k} - \mathbf{q}, \Delta E)$ reads

$$\begin{aligned} S_{\alpha\beta}^{\text{in}} &= \sum \frac{2\pi}{\hbar} |V(q, \Delta E)|^2 [1 - f_\beta(\mathbf{k}', t)] f_\beta(\mathbf{k}' + \mathbf{q}) \delta(X), \\ S_{\alpha\beta}^{\text{out}} &= \sum \frac{2\pi}{\hbar} |V(q, \Delta E)|^2 f_\beta(\mathbf{k}', t) [1 - f_\beta(\mathbf{k}' + \mathbf{q}, t)] \delta(X). \end{aligned} \quad (5)$$

Here, $\delta(X) = E_\alpha(\mathbf{k}) + E_\beta(\mathbf{k}') - E_\alpha(\mathbf{k} - \mathbf{q}) - E_\beta(\mathbf{k}' + \mathbf{q})$ and $\Delta E = E_\alpha(\mathbf{k}) - E_\alpha(\mathbf{k} - \mathbf{q})$. We recover immediately the standard form of the scattering integral due to carrier-carrier interaction [for example, formula (4) in Ref. 5]. The definite form of $V(q, \Delta E)$ will be discussed hereafter. To extend significantly our previous treatment,⁵ we must take into account the carrier damping [$\Gamma_c(\mathbf{k}, t)$ for electrons and $\Gamma_v(\mathbf{k}, t)$ for holes] which just results from the carrier scattering by the different processes considered above. For instance, the electron damping reads

$$\Gamma_c(\mathbf{k}, t) = \Gamma_{cc}(\mathbf{k}, t) + \Gamma_{cv}(\mathbf{k}, t) + \Gamma_{c,LO}(\mathbf{k}, t). \quad (6)$$

Here, $\Gamma_{cc}(\mathbf{k}, t)$ is the damping due to electron-electron collisions, $\Gamma_{cv}(\mathbf{k}, t)$ is the damping due to electron-hole collisions, and $\Gamma_{c,LO}(\mathbf{k}, t)$ is due to inelastic scattering by LO phonons. For each process the damping is given by

$$\begin{aligned} \Gamma_{\alpha\beta}(\mathbf{k}, t) &= \sum_q S_{\alpha\beta}^{\text{out}}(\mathbf{k}, \mathbf{k} - \mathbf{q}, \Delta E) [1 - f_\alpha(\mathbf{k} - \mathbf{q}, t)] \\ &\quad + S_{\alpha\beta}^{\text{in}}(\mathbf{k}, \mathbf{k} - \mathbf{q}, \Delta E) f_\alpha(\mathbf{k} - \mathbf{q}, t). \end{aligned} \quad (7)$$

$\Gamma_c(\mathbf{k}, t)$ depends on time because we use the transient non-equilibrium distribution functions when calculating each $\Gamma_{\alpha\beta}$ component. Equation (7) is the generalization to the nonequilibrium case of the carrier damping which can be deduced as the imaginary part of the carrier self-energy at thermodynamical equilibrium.^{12,13} $\Gamma_c(\mathbf{k}, t)$ is expected to increase during the excitation pulse if the carrier-carrier scatterings become comparable to, or more efficient than, the inelastic LO-phonon scattering as a result of the increase of the plasma density. The carrier damping plays a critical part in broadening the energy range of carriers that can interact with light, both during the plasma generation in the optical pumping step and thereafter with any probe pulse in case of picosecond transmission

spectroscopy. Let us consider a quasimonochromatic pump pulse at the central frequency ν . We will assume a Gaussian-like time behavior of the pump power. Provided the spectral flux envelope function ϕ_ν varies slowly

with respect to ν [i.e., that the following condition $(1/\phi_\nu)(d/dt)\phi_\nu < \nu$ holds], the electron-hole pair generation rate may be written as

$$g(\mathbf{k}, \nu, t) = \alpha_0 \frac{\phi_\nu(t)}{h\nu} [1 - f_c(\mathbf{k}) - f_v(\mathbf{k})] \left[\frac{\hbar^2}{2\mu} \right]^{3/2} \frac{\frac{2}{\pi} \hbar [\Gamma_c(\mathbf{k}, t) + \Gamma_v(\mathbf{k}, t)]}{[h\nu - E_G - (\hbar^2/2\mu)k^2]^2 + \hbar^2 [\Gamma_c(\mathbf{k}, t) + \Gamma_v(\mathbf{k}, t)]^2} . \quad (8)$$

$\alpha(h\nu)$ is a material parameter. It depends on the plasma concentration. The band-gap shrinkage tends to increase $\alpha(h\nu)$ due to the increase of the state density. On the other hand, the reduction of the excitonic enhancement leads to a decay of the free-carrier absorption close to the band gap at high plasma density. In the experiments which we will consider, this effect will be neglected around the pump energy. This point will be discussed in Sec. III. We account broadly for the spectral bandwidth of the laser pump around the central frequency ν by summing over all the pump frequencies. The generation rate $g_\lambda(\mathbf{k}, t)$ [formula (2)] and the absorption coefficient α read, respectively,

$$g_\lambda(\mathbf{k}, t) = \int_0^{+\infty} g(\mathbf{k}, \nu, t) d(h\nu) , \quad (9a)$$

$$\alpha(h\nu) = \int \frac{h\nu}{\phi_\nu(t)} g(\mathbf{k}, \nu, t) d^3k . \quad (9b)$$

In relation (9a), the Gaussian envelope function $\phi_\nu(t)$ is convoluted with the Lorentzian function due to the damping displayed in formula (8). The net effect is that the carrier generation becomes less resonant than is expected by the wave-vector selection rule. In formula (9b), the occupation function $[1 - f_c(\mathbf{k}) - f_v(\mathbf{k})]$ is also convoluted with the Lorentzian function of formula (8). Let us discuss now the renormalization of the carrier-carrier and carrier-LO-phonon interactions which appear in the quantity $S(\mathbf{k}, \mathbf{k}-\mathbf{q}, \Delta E)$ of formula (4). All the interactions must be renormalized in the presence of the electron-hole plasma generated by the excitation pulse because of the plasma polarizability. We account (partly) for this effect by introducing the plasma dielectric function $\epsilon(q, \omega)$. We write down the scattering amplitude in formula (5) as follows:

$$V(\mathbf{q}, \omega) = \frac{V_0(q)}{\epsilon(\mathbf{q}, \Delta E/\hbar)} . \quad (10)$$

Here $V_0(q)$ is the bare interaction (carrier-carrier or carrier-phonon interaction). We refer to Ref. 5 for more details on the bare interactions. \mathbf{q} and ΔE are, respectively, the wave vector and the energy exchanged between the carrier and the second quasiparticle in the collision process. It seems very appealing to use the plasma dielectric function calculated in the random-phase approximation (RPA) formally extended to athermal systems.¹⁴ This theory, as modified by Hubbard,¹⁵ leads to good quantitative results in metal and semiconductor physics (see, for example, Mahan for a general review of the RPA theory.¹⁶ However, this approach is not yet possible because the resolution of system (2) can be performed only

numerically and computer capabilities seem (for the moment) too low for solving this system using the full RPA dielectric function, especially when describing the carrier-carrier scatterings.¹⁷ So the central problem in plasma dynamics description is to find a satisfying compromise between the refinements in the theory of kinetic equations and the refinements in the scattering amplitude aspects, which enables the computer processing of the equations. In a first step, we resign ourselves to the static approximation, i.e., we assume that the energy ΔE exchanged in the most probable scattering processes is very small. Then the dielectric function reduces to the following simple analytical form:

$$\epsilon(q, 0) = 1 + \frac{q_{\text{DH}}^2}{q^2} . \quad (11)$$

q_{DH} is the Debye-Huckel wave vector calculated using nonequilibrium distribution functions. q_{DH}^2 reads

$$q_{\text{DH}}^2 = \frac{-4\pi e^2}{\epsilon_\infty} \lim_{q \rightarrow 0} \left[\sum_{\mathbf{K}, \alpha} \frac{f_\alpha(\mathbf{K} + \mathbf{q}) - f_\alpha(\mathbf{K})}{E_\alpha(\mathbf{K} + \mathbf{q}) - E_\alpha(\mathbf{K}) + i\eta} \right] . \quad (12)$$

In the following we will also use an effective screening length $q_{\text{eff}}^2 = Cq_{\text{DH}}^2$ with $C < 1$ to discuss the screening.

For the numerical treatment, each quasiparticle distribution (conduction, valence, and LO-phonon) is sampled typically over 50 points. Kinetic equations (2)–(12) are solved numerically step by step using a fifth-order predictor-corrector routine (two-thirds case; see, for instance, (Ref. 18). Further information on the numerical aspects can be found in Ref. 5. The program runs on a Micro-VAX II computer. The CPU time to calculate the kinetics over 1 ps is about 10 h.

III. COMPARISON WITH EXPERIMENTS: SCREENING EFFICIENCY

Absorption saturation on a subpicosecond time scale was recently observed in Ref. 2 and also suggested in Ref. 5. We will test the model by comparing these experimental results to the numerical calculations. First, we summarize briefly the experimental conditions and the experimental results of Ref. 2. A pump pulse of 0.5 ps duration [full width at half maximum (FWHM)] and 5 meV spectral bandwidth was used to excite electron-hole pairs at the energy 1.538 eV in a thin GaAs sample maintained at a temperature of 15 K. This energy was only 19 meV above the band gap of the unexcited GaAs sample, so that the initial kinetic energy of each electron or each hole was

smaller than that of the optical phonon. In this way, the dominant scattering mechanism was that of carrier-carrier interactions which are fully taken into account in the present calculation. With a white light continuum pulse of 0.1 ps duration, transmission spectra could be recorded at various time delays, with the help of a grating spectrometer followed by an optical multichannel analyzer. The experimental results are reported in Fig. 1 (solid line) together with the computed spectra obtained from our model. In the calculations, we used the set of physical parameters listed in Table I, both for the material and the excitation laser pulse. The pulse peak power is the only adjustable parameter which is available for fitting simultaneously all the experimental spectra. As displayed in Fig. 1, the fits around the pump photon energy, i.e., in the energy range extending from 1.52 to 1.56 eV, are very good. We used first the static screening. The model accounts accurately for the amplitude of the absorption saturation over 1.4 ps which is the new experimental effect reported in Ref. 2 and is the purpose of the present investigation. We did not attempt to fit the dynamics of the absorption coefficient $\alpha(h\nu)$ below the energy 1.52 eV, especially around the band-gap energy achieved in the experiment which is typically $E_G \sim 1.505$ eV at the peak density $p = 3 \times 10^{17}$ cm $^{-3}$. In this energy range, the absorption of the probe by the free carriers is influenced by the reduction of the excitonic enhancement and the band-gap shrinkage which take place at high plasma density. This effect, not included in our calculation, is, however, small around the photon pump energy, which is $E_p = 1.538$ eV. This is clearly demonstrated by previous nanosecond-technique experiments reported on GaAs:¹⁹ The observed absorption coefficient is not really density dependent (up to a plasma density of 1.5×10^{17} cm $^{-3}$) when the photon energy is higher than 1.532 eV. There is

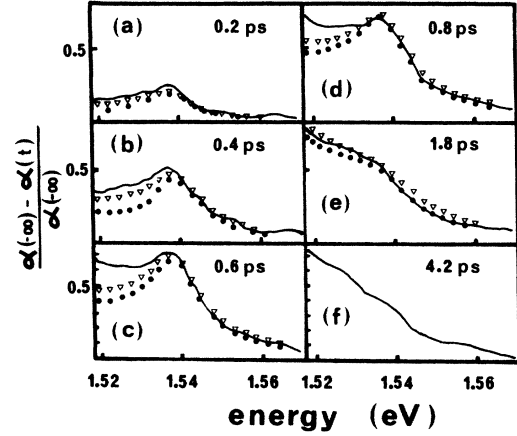


FIG. 1. Solid line: experimental results. Time-resolved transmission spectra $[\alpha(-\infty) - \alpha(t)]/\alpha(-\infty)$ [where $\alpha(-\infty)$ is the unperturbed absorption coefficient] for different time delays between the pump and the probe. (a) Delay=0.2 ps; (b) delay=0.4 ps; (c) delay=0.6 ps; (d) delay=0.8 ps; (e) delay=1.8 ps; (f) delay=4.2 ps. Dotted line: model calculation using static screening. Peak pump power: 35 MW/cm 2 . (a) Density: 5.0×10^{16} cm $^{-3}$; (b) density: 1.54×10^{17} cm $^{-3}$; (c) density: 2.1×10^{17} cm $^{-3}$; (d) density: 2.91×10^{17} cm $^{-3}$; (e) density: 3.05×10^{17} cm $^{-3}$. Triangles: model calculation using the quasi-static screening ($C=0.85$).

no reason to assume that the excitonic enhancement change might be suddenly the dominant effect responsible for bleaching just at the pump energy when the density reaches 3×10^{17} cm $^{-3}$. In other words, the absorption saturation observed at the energy 1.538 eV is due to state filling. The impact of the excitonic enhancement variation

TABLE I. Physical parameters used in the model calculation.

GaAs parameters		Excitation pulse parameters	
Static dielectric function (cgs)	12.6	Time duration at half maximum (ps)	0.5
Infinite dielectric function (cgs)	11	Spectral bandwidth at half maximum (meV)	5
LO-phonon energy (eV)	36	Photon energy (eV)	1.538
Conduction mass	0.066	Peak pulse power (MW/cm 2)	adjustable
Valence-band mass	0.57		
Absorption coefficient (10^4 cm $^{-1}$ eV $^{-1/2}$) ^a	4.4		
Band-gap renormalization coefficient (10^{-8} eV cm) ^b	2.15		
Band-gap energy (eV)	1.519		

^aReference 23.

^bReference 26.

becomes critical at lower pump energy. We did not attempt to fit the last spectrum at time 4.2 ps to save computation time, which could last up to 20 h. It is, however, obvious that if the model fits the spectrum at time 1.8 ps, it must also fit the thermalized spectrum at time 4.2 ps. The model also fits the broadening of the saturation peaks of the different spectra. This is also a significant result because there is *a priori* no parameter in the model²⁰ to adjust the broadening. The whole series of computed spectra depends critically on the efficiency of the scattering processes. We can test the sensitivity to screening by introducing the phenomenological wave vector $q_{\text{eff}}^2 = Cq_{\text{DH}}^2$. If we assume $C=0.85$ (triangles in Fig. 1), the fits at short delays are somewhat improved, but the long delay spectrum at time $t=1.8$ ps is fitted with difficulty because the nonthermalized bump around 1.538 eV becomes less pronounced in the computed kinetics. It must be stressed that the spectrum at time 1.8 ps is extremely important because it represents a critical test of the efficiency of the carrier-carrier scattering processes on a long-time scale (i.e., 1 ps). If we assume $C=0.7$ (not reported in Fig. 1), the fit of the first spectra is still improved around 1.52 eV (however, this is meaningless because of the excitonic effects). More basically, the long delay spectrum at time $t=1.8$ ps cannot be fitted because the nonthermalized bump around 1.538 eV disappears in the calculations. This demonstrates that scatterings are overestimated in this approximation. If we suppress almost completely the screening by assuming a small screening wave vector (say, $C=0.2$), no absorption saturation appears in the computed kinetics. Thermalization is quasi-instantaneous. We may conclude that the static screening (i.e., $C=1$) or the quasistatic screening (i.e., $C=0.9$) lead to satisfying results in describing the plasma dynamics when the pump energy is lower than the band-gap energy plus one LO phonon. We put forward *a posteriori* the following explanation: The high sensitivity of the computed kinetics to any adjustment of the screening wave vector q_{DH} demonstrates that the most probable (and therefore the most efficient) carrier-carrier scatterings are characterized by the exchange of a small vector q with respect to q_{DH} . In other words, the energy exchanged in the more frequent collisions is small compared to the plasmon energy. This is very reasonable since the average energy of electrons or holes is low (always lower than 27 meV), while the plasmon energy is higher than 20 meV in GaAs for the density range larger than $2 \times 10^{17} \text{ cm}^{-3}$ quickly achieved [before the spectrum (c) in Fig. 1] in the experiment under consideration. So it turns out that for the most efficient scattering processes, the dielectric function reduces to the static limit $\epsilon(q,0)$ and therefore the static approximation holds. The plasma densities are very close to the values deduced previously.² These transmission spectra are of course deduced from the preliminary calculation of the kinetics, both of the quasiparticle distributions (conduction, valence, and LO phonon) and dampings. These kinetics are displayed in Figs. 2–4. We comment on each one briefly.

(i) *Electrons in the conduction band* [Fig. 2(a)]. The x-axis label is the kinetic energy of electrons. During the excitation step the band gap shrinks as a result of the

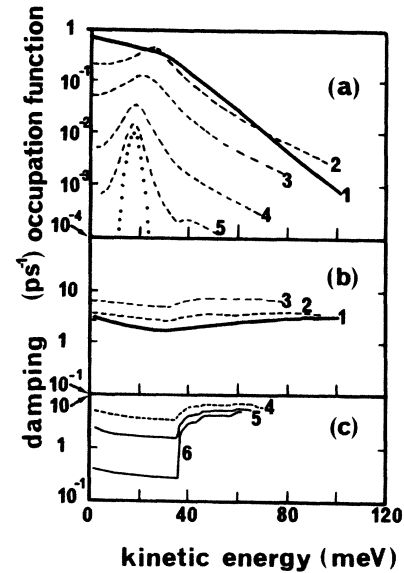


FIG. 2. (a) Kinetics of electrons in the conduction band. The dotted line represents the laser pulse broadening. (b) and (c) conduction-band damping. 1. delay: 1.77 ps; 2. delay: 0.49 ps; 3. delay: 0.19 ps; 4. delay: 0.0 ps; 5. delay: -0.1 ps; 6. delay: -0.2 ps. The peak excitation is at time 0.45 ps.

plasma density increase. Therefore, the initial kinetic energy of the generated electrons increases. This is clearly displayed in Fig. 2(a) by the shift of the generation peak toward high energy during the kinetics. The spectral bandwidth of the laser pump is represented by the dotted line.

(ii) *Conduction damping* [Figs. 2(b) and 2(c)]. At the beginning of the kinetics (time $t < -0.1$ ps), the plasma density is still weak so that the contribution to the damping of carrier-carrier collisions is very low compared to

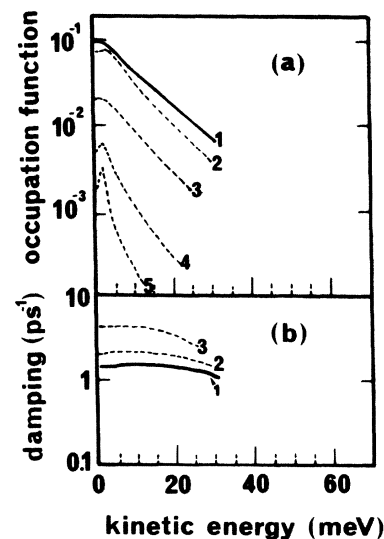


FIG. 3. (a) Kinetic energy of holes in the valence band. (b) Hole damping. 1. delay: 1.77 ps; 2. delay: 0.49 ps; 3. delay: 0.19 ps; 4. delay: 0.0 ps; 5. delay: -0.1 ps. The peak excitation pulse is at time 0.45 ps.

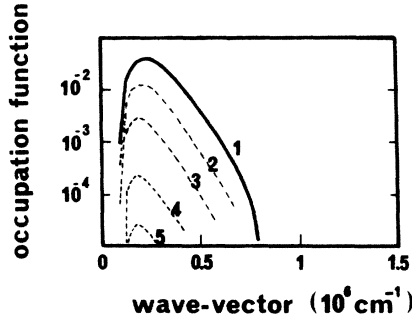


FIG. 4. Kinetics of LO phonons. 1. Delay: 1.77 ps; 2. delay: 0.49 ps; 3. delay: 0.19 ps; 4. delay: 0.0 ps; 5. delay: -0.1 ps. The peak excitation pulse is at time 0.45 ps.

the contribution of LO-phonon scatterings. It results in the damping being weak for electrons in which the kinetic energy is less than one LO phonon ($\hbar\omega_{LO} = 36$ meV). On the contrary, the damping quickly becomes strong (due to the possible emission of LO phonons) if the kinetic energy is higher than 36 meV. Typically, for these carriers of high kinetic energy, the damping Γ_c is of the order of 250 ps, which is in good agreement with the usual value reported in the literature.^{21,22} Under laser excitation, the damping of all the electrons increases quickly due to the increase of the carrier-carrier scattering rate. However, for time longer than 200 fs, the damping decreases. This effect, which is surprising at first sight, is due to the screening which reduces the scattering amplitudes [formula (10)] and also to the degeneracy which appears in the quasiparticle distribution (i.e., the sum $f_c(\mathbf{k}) + f_v(\mathbf{k})$ no more is negligible with respect to 1). It turns out that the conduction damping becomes weakly dependent on the carrier kinetic energy and time delay for instants longer than 0.5 ps.

(iii) *Holes in the valence band* [Fig. 3(a)]. The x -axis label is the hole kinetic energy. The initial kinetic energy of holes is small compared to that of electrons in the conduction band (typically $E_v/E_c = m_c/m_v$). During the transient regime, holes gain kinetic energy through collisions with electrons. This is clearly displayed in Fig. 3(a). However, it must be stressed that the average electron kinetic energy $\langle E_c \rangle$ remains significantly higher than the average hole kinetic energy $\langle E_v \rangle$ over the whole analyzed regime. At time $t = 1.8$ ps, $\langle E_c \rangle$ and $\langle E_v \rangle$ are, respectively, equal to 25 and 15 meV, so that the ratio $\langle E_c \rangle / \langle E_v \rangle$ is 1.7.²³

(iv) *Hole damping* [Fig. 3(b)]. The hole damping behaves like the electron one. First we observe that it increases (delay $t < 0.2$ ps) but thereafter decays. The electron-hole pair damping (i.e., $\Gamma_c + \Gamma_v$) which appears in Eq. (8) becomes also weakly dependent on the pair kinetic energy and on the plasma density ($p > 10^{17}$ cm $^{-3}$ and $t > 0.4$ ps), in agreement with the assumptions of Ref. 2.

(v) *LO-phonon distribution* (Fig. 4). This distribution is also computed within the program. In the present case of pumping which creates electron-hole pairs of low kinetic energy, the occupation of the LO-phonon modes close to

the Brillouin-zone center remains small and does not really influence the carrier kinetics (in contrast to the results reported, for example, in Ref. 5). In other words, the possible reabsorption of nonequilibrium phonons by the carriers is negligible here. This justifies *a posteriori* the assumption that TO phonons, less coupled than LO phonons to the plasma, do not influence the carrier kinetics.

IV. ABSORPTION SATURATION AT SHORTER WAVELENGTH

We used our model calculation to investigate the possibility of absorption saturation higher in the bands when the material is pumped by a radiation at shorter wavelength. We keep the static approximation. The computed time-resolved spectra $[\alpha(-\infty) - \alpha(t)] / \alpha(-\infty)$ are reported in Fig. 5 for two typical excitation wavelengths, namely, $\lambda = 790$ and 770 nm. In the first case, each electron in the conduction band can emit one LO phonon, while it can emit two LO phonons in the second case. We conclude from our calculations that absorption saturation should be accessible experimentally (as clearly evidenced in Fig. 5). The variation of the excitonic enhancement is expected to be very weak at the pump energies under consideration.

V. CONCLUSION

In this work we report, to the best of our knowledge, the first comparison of experimental results of subpicosecond spectroscopy to a theory of athermal plasma dynamics. We can fit easily the experimental series of absorption saturation spectra reported in Ref. 2 over 1.6 ps without introducing any phenomenological parameter. Screening efficiency is discussed. We conclude that the static screening approximation is satisfying for describing

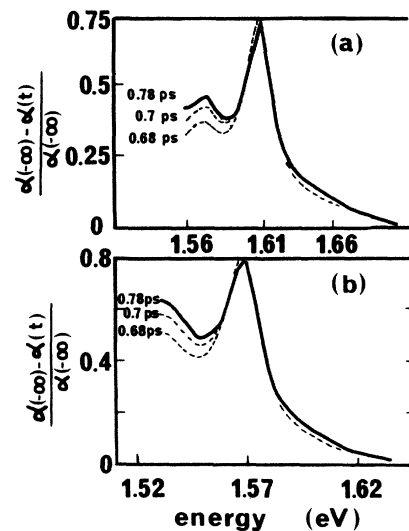


FIG. 5. Computed absorption saturation kinetics in case of laser excitation with photons of higher energy. The peak excitation power is 80 MW/cm 2 . (a) Excitation wavelength: 770 nm. (b) Excitation wavelength: 790 nm.

the main scattering processes in a high-density plasma close to the band gap. This is the standard approximation in transport theory.^{24,25} Carrier dampings are also calculated and discussed. They must be absolutely included. Previous calculations⁵ without dampings overestimated strongly the absorption saturation and could not account for the experimental results. The absorption saturation at the pump energy 1.538 eV is due to state filling, which is controlled by the carrier scatterings. We have also concluded that thermalization between electrons and holes cannot be achieved at the end of the analyzed regime, i.e., 1.4 ps after the peak of the 0.5-ps excitation pulse. Finally, the possibility of absorption saturation experiments using photons of higher energy is discussed. Although fur-

ther investigations are still desirable to test dynamical screening in kinetic equations or to resolve more general master equations, this work demonstrates that a significant progress has been realized towards a quantitative theory of the athermal dynamics of electrons, holes, and LO phonons on a picosecond or subpicosecond time scale.

ACKNOWLEDGMENTS

The numerical programs of this work have been run at the Service d'Informatique de l'Institut National des Sciences Appliquées, Toulouse, which we acknowledge for its support. We thank especially Mr. D. Nicolas for his assistance.

-
- ¹R. F. Leheny, J. Shah, R. L. Fork, C. V. Shank, and A. Migus, *Solid State Commun.* **31**, 809 (1979).
- ²J. L. Oudar, D. Hulin, A. Migus, and A. Antonetti, *Phys. Rev. Lett.* **55**, 2074 (1985).
- ³D. Von der Linde, J. Kuhl, and H. Klingenberg, *Phys. Rev. Lett.* **44**, 1505 (1980).
- ⁴J. A. Kash and J. Tsang, *Phys. Rev. Lett.* **54**, 2151 (1985).
- ⁵J. Collet and T. Amand, *Phys. Chem. Solids* **47**, 153 (1986).
- ⁶When the LO-phonon scattering becomes less efficient at high density, one more equation must be included for the TO-phonon emission. See, W. Potz and P. Kocevar, *Phys. Rev. B* **28**, 7040 (1983).
- ⁷L. O. Kadanoff and G. Baym, *Quantum Statistical Mechanics* (Benjamin, New York, 1962).
- ⁸V. Keldish, *Zh. Eksp. Teor. Fiz.* **47**, 1515 (1964) [*Sov. Phys.—JETP* **20**, 1018 (1965)].
- ⁹A. G. Hall, *Physica A* **80**, 369 (1975).
- ¹⁰E. M. Lifshitz and L. P. Pitaevskii, *Course of Theoretical Physics*, Vol 10 of *Physical Kinetics* (Pergamon, New York, 1981).
- ¹¹J. H. Collet and T. Amand, *Phys. Rev. B* **33**, 4129 (1986).
- ¹²G. D. Mahan, in *Polarons in Ionic Crystals and Polar Semiconductors*, edited by J. T. Devreese (North-Holland, Amsterdam, 1972), p. 633.
- ¹³H. Haug and D. B. Tran Thoai, *Phys. Status Solidi B* **98**, 591 (1980).
- ¹⁴H. Ehrenreich and M. H. Cohen, *Phys. Rev.* **115**, 786 (1959).
- ¹⁵J. Hubbard, *Proc. R. Soc. London, Ser. A* **243**, 336 (1957).
- ¹⁶G. D. Mahan *Many Particle Physics* (Plenum, New York, 1983).
- ¹⁷The carrier—LO-phonon interaction is simpler (Fröhlich interaction) and could be worked out in the full RPA treatment.
- ¹⁸R. W. Hamming, *Numerical Methods for Scientists and Engineers* (McGraw-Hill, New York, 1962), p. 206.
- ¹⁹J. Shah, R. F. Leheny, and W. Wiegmann, *Phys. Rev. B* **16**, 1577 (1977).
- ²⁰We tried first to fit the experimental spectra using our previous model (Ref. 5), which does not take into account the carrier dampings. Fits are unsatisfactory. Basically, the intensity of the saturation absorption is overestimated, while the saturation peak around 1.538 eV is too narrow. This stresses the critical part of damping in the theory.
- ²¹E. M. Conwell, *High Field Transport in Semiconductors* (Academic, New York, 1967).
- ²²D. N. Mirlin, I. J. Karlik, L. P. Nikitin, I. I. Reshina, and U. P. Sapega, *Solid State Commun.* **37**, 757 (1981).
- ²³As was recently pointed out by M. Asche and U. G. Sarbei, in *Phys. Status Solidi B* **126** 607 (1984), a possible temperature difference between electrons and holes cannot be discarded and may reduce the plasma energy-loss rate at high density. This is also supported by our former calculations (Ref. 5). However, all of our results suggest that thermalization can hardly be achieved before 0.8 ps (Ref. 5), neither for electrons nor (to some extent) for holes. We found also that holes significantly gain kinetic energy from electrons during the first picosecond. We emphasize that the first picosecond must be investigated using athermal distribution functions.
- ²⁴C. Jacobini, *Hot Electron Transport in Semiconductors* (Springer-Verlag, Berlin, 1985).
- ²⁵R. Barker, in *Physics of the Non Linear Transport in Semiconductors*, edited by D. K. Ferry (Plenum, New York, 1979).
- ²⁶T. Amand and J. H. Collet, *Phys. Chem. Solids* **46**, 1053 (1985).